

Coefficient-Guided Chebyshev–PCHIP Approximation for Mixed-Regularity Functions

Hameed Hasan Obaid Yasari
Assistant Lecturer, Field of Mathematical Analysis, General Directorate of Education in the Holy Karbala Governorate, Karbala, Iraq

* Corresponding Author: **Hameed Hasan Obaid Yasari**

Article Info

ISSN (Online): 3107-6580
Volume: 01
Issue: 06
Received: 25-10-2025
Accepted: 27-11-2025
Published: 22-12-2025
Page No: 70-82

Abstract
In this paper we propose and evaluate a coefficient-decay-triggered hybrid approximation for one-dimensional functions with changing regularity in their domain. If the coefficient-tail indication and independent validation residual are small, local Chebyshev interpolation is appropriate; otherwise the interval is recursively bisected. Shape-preserving cubic piecewise Hermite interpolation (PCHIP) reconstructs consistently uneven end intervals. A jump classifier activates one-sided PCHIP pieces to prevent misleading continuous transitions. validation guided, practical acceptance test, not an a posteriori limit, the off-grid residual. The five deterministic benchmarks are analytic, cusp, algebraic-singularity, jump and mixed regularity. The proposed method is benchmarked against global Chebyshev interpolation, global PCHIP, cubic splines, and an adaptive Chebyshev-only baseline. On the mixed benchmark it achieves RMSE 1.41×10^{-5} versus adaptive Chebyshev (5.24×10^{-3}), global Chebyshev (2.28×10^{-2}), and global PCHIP (2.13×10 At a construction budget of 1,317 function evaluations, global Chebyshev, PCHIP, and cubic splines hold RMSE levels of 1.07×10^{-2}, 6.00×10^{-3}, and 6.56×10^{-3}, respectively, whereas the hybrid representation holds only 344 degrees of freedom Global Chebyshev still dominates the analytic benchmark, showing that switching is generally advantageous when regularity is spatially nonuniform. Sensitivity studies demonstrate that the baseline mixed-function partition is insensitive to tail thresholds of 3×10^{-5} to 10^{-2} and three to eight tail coefficients The jump classifier identifies 20 piecewise-constant leaps across five locations and four amplitudes after automatic bracketing, whereas selected non-jump controls are not misclassified for thresholds 4 to 24. Instead of substituting the spectral approximation, we propose a regularity dependent validation guided switching approach.

DOI: https://doi.org/10.54660/.IJECA.2025.1.6.70-82

Keywords: Chebyshev approximation, PCHIP, coefficient decay, adaptive approximation, mixed regularity

1. Introduction

Chebyshev interpolation is a classical, high precision approach for smooth functions over a confined interval. Chebyshev-Lobatto nodes do not have the crowding around the endpoints, the barycentric evaluation is numerically stable and analytic functions may converge geometrically or faster (Berrut & Trefethen, 2004; Trefethen, 2019) [7, 15]. A function with a cusp, algebraic singularity, or jump has a different regime. Coefficient decay becomes algebraic, the rate of global convergence drops, and the largest pointwise errors are located near the loss of regularity. Such behavior has been quantified for singular and limited-regularity functions in fractional-space settings (Liu *et al*., 2019; Wang, 2023; Zhang & Boyd, 2023; Xie, 2026) [13, 16, 17, 18]. Adaptive polynomial techniques modify the resolution or the domain structure. In piecewise-smooth Chebfun representations we use recursive subdivision and local Chebyshev expansions; domain-splitting analysis shows that when singularities limit the

Bernstein ellipse, piecewise interpolation is more efficient than a global polynomial (Pachon *et al*., 2010; Driscoll & Weideman, 2014. Chebfun's coefficient-chopping technique shows how the numerical tail of a Chebyshev series may influence resolution choices without symbolic smoothness information (Aurentz & Trefethen, 2017) [5]. In recent hp-adaptive research, the coefficient behavior is also used for the selection of local refinement techniques (Drozd *et al*., 2024) [9].

A second line of work modifies approximation families around troublesome features. Maintaining monotonicity cubic For the purpose of eliminating artificial extrema in data that are locally monotone, Hermite interpolation is used. The mathematical foundation of PCHIP-type algorithms is given by the basic conditions, local construction, and error analysis of Fritsch and Carlson (1980) [11], Fritsch and Butland (1984) [10], and Huynh (1993) [12]. 5. Monotonicity-preserving interpolation, utilized in modern multilevel calculations, describes abrupt variations without oscillatory reconstruction (Baeza *et al*., 2024) [6].

This study combines these principles selectively. The degradation of the local coefficient and the off-grid validation show that the high-order polynomial approximation is effective. Therefore, the Chebyshev interpolation is retained. Only chronically uneven terminal intervals are sent to PCHIP. The final representation may be discontinuous, due to a separate jump classifier, which is needed since a shape-preserving continuous interpolant placed across a discontinuity would blur a true jump. What is new here is not Chebyshev approximation or PCHIP per se, but a means of automatically switching between them, using local spectral behavior as a signal to refine the subdomain, and changing the approximation family only after repeated failures of the Chebyshev acceptance test.

We developed a numerical research. Its goals are to (i) test localization of nonsmooth features, (ii) employ an adaptive Chebyshev-only control to separate the benefits of switching families and subdivision, (iii) compare accuracy at equal representation size and construction budget, and (iv) test sensitivity to coefficient-tail threshold, number of tail coefficients, jump threshold, local polynomial degree, PCHIP resolution, recursive depth and post-hoc exclusion ra The article does not claim a strict global error bound as the validation residual is sampled rather than verified. Future work entails deriving such a restriction.

2. Analytical and Numerical Background

2.1. Local Chebyshev Representation

On a subinterval I=[a,b], define t=(2x-a-b)/(b-a). A degree-m local Chebyshev interpolant is

$$p_m(x) = \Sigma(k=0,\ldots,m)\ a_k T_k(t),\ t = (2x-a-b)/(b-a).$$

Function values are sampled at Chebyshev-Lobatto points and the coefficients are obtained by a type-I discrete cosine transform. For analytic functions the coefficients decay rapidly, whereas limited regularity produces slower algebraic decay. This is why coefficient magnitude can serve as a local resolution diagnostic (Liu *et al*., 2019; Trefethen, 2019; Wang, 2023) [13, 15, 16]. Recent pointwise analysis further shows explicit dependence of Chebyshev error on singularity strength and distance from the singularity (Xie *et al*., 2026) [17].

2.2. Coefficient-Tail Indicator and Validation Residual

For coefficients a_0,...,a_m, define the relative tail indicator

$$\rho_i = [\Sigma(k=m-q+1,\ldots,m)\ |a_k|] / [\Sigma(k=0,\ldots,m)\ |a_k| + \varepsilon].$$

A small ρ_i means that the retained polynomial has entered a decaying tail; a large value indicates unresolved high-order content. Tail-based decisions are consistent with coefficient-chopping and hp-adaptive ideas in the literature, although the present ratio is intentionally simpler than Chebfun's full chopping logic (Aurentz & Trefethen, 2017; Drozd *et al*., 2024) [5, 9]. To prevent a small tail ratio from being accepted when the polynomial is still inaccurate, an off-grid validation residual is computed:

$$e_i = \max(x\in V_i)\ |f(x)-p_m(x)| / \max[1, \max(x\in V_i)|f(x)|].$$

An interval is accepted as a Chebyshev leaf only if $\rho_i <= tau$ and $e_i <= tol$. Otherwise it is bisected. The residual is a deterministic validation criterion, not a certified supremum-norm bound; therefore the algorithm is described as validation-guided rather than error-controlled.

2.3. PCHIP Switching and Jump-Aware Reconstruction

An interval still failing the Chebyshev test is recreated using PCHIP at the highest recursive depth . We choose this local monotone cubic family as it eliminates the spurious extrema that may appear in unrestricted cubic interpolation of monotone data (Fritsch & Carlson, 1980; Fritsch & Butland, 1984) [10, 11]. It is not meant as a spectral substitution, since its order may be decreased at extrema due to the monotonicity restriction; it is a local defensive representation for intervals when high-order Chebyshev behavior has already failed (Huynh, 1993) [12].

To distinguish a true jump from a continuous irregularity, terminal samples y_i are assigned the score

$$J_i = \max_i\ |y_{i+1}-y_i| / [\text{median}_i\ |y_{i+1}-y_i| + \varepsilon].$$

If J_i exceeds J*, the largest first difference brackets a potential jump. Bisection then refines the split location, after which independent left and right PCHIP pieces are constructed. Importantly, the extremely small location errors reported later measure post-bracketing bisection refinement in deterministic step tests; they should not be interpreted as a general statistical detection accuracy.

2.4. Position Relative to Previous Work

The proposed scheme differs from piecewise Chebyshev approaches because terminal irregular intervals are permitted to change approximation family rather than remaining polynomial (Pachon *et al*., 2010; Driscoll & Weideman, 2014) [8, 14]. It also differs from Padé-Chebyshev approaches for nonsmooth functions, where the nonlinear rational family is used to suppress Gibbs behavior without a Chebyshev-to-PCHIP switch (Akansha, 2024b; Akansha, 2025) [2, 3]. Work on coefficient decay and error estimates for limited-regularity functions provides the theoretical motivation for using spectral tails as a diagnostic, but it does not prescribe the hybrid switching rule studied here (Akansha, 2024a; Akansha & Subramaniam, 2025) [1, 4].

3. Numerical Methodology

3.1. Reproducible Workflow

Table 1: Validation-guided hybrid approximation workflow.

Step	Operation
1	Start with I=[-1,1] and sample m+1 Chebyshev-Lobatto points.
2	Compute local Chebyshev coefficients, ρ_i, and the independent validation residual e_i.
3	Accept a Chebyshev leaf if ρ_i<=tau and e_i<=tol.
4	Otherwise bisect while depth<dmax and repeat the local test.
5	At terminal depth compute the local jump score J_i.
6	If J_i>=J*, bracket and refine the jump by bisection, then fit one-sided PCHIP pieces.
7	Otherwise fit a single PCHIP interpolant on the irregular leaf.
8	Assemble all Chebyshev and PCHIP leaves into a piecewise global representation.

Table 2: Baseline numerical parameters.

Parameter	Baseline value
Local Chebyshev degree m	20
Tail coefficients q	5
Tail threshold tau	1e-3
Validation tolerance tol	1e-7
Maximum depth dmax	8
PCHIP nodes on non-jump leaf	17
Local samples for jump classification	33
Jump-score threshold J*	8
Bisection iterations	20
Error grid	200,000 midpoint samples
Regular-region exclusion radius delta	0.02

3.2. Benchmark Functions

Table 3: Benchmark functions and regularity classes.

Test	Definition	Role
Smooth	exp(0.3x) sin(5x)+0.1 cos(11x)	Analytic control
Cusp	|x-0.17|	Derivative jump at 0.17
Weak singularity	sqrt(|x+0.33|)	Algebraic singularity at -0.33
Step	0 for x<0.13; 1 otherwise	Single jump at 0.13
Mixed	0.35 sin(6x)+0.45|x+0.41|^0.65+0.70H(x-0.23)+0.08 cos(15x)	Cusp at -0.41 and jump at 0.23

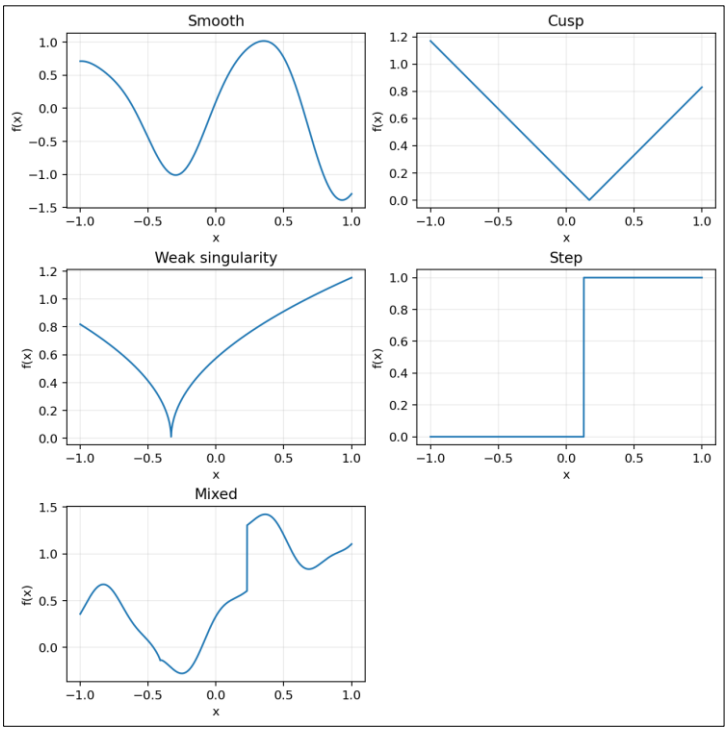


Fig 1: Benchmark functions used in the numerical study.

3.3. Comparison Methods and Metrics

The proposed hybrid is compared with four controls: adaptive Chebyshev using the same subdivision logic but no family switch, global Chebyshev interpolation, global PCHIP, and a natural cubic spline. In the primary comparison the global methods receive the same stored representation size as the hybrid method for that benchmark. A second comparison on the mixed benchmark gives the global methods the same construction budget as the hybrid method, addressing the possibility that the adaptive method benefits merely from more function evaluations.

The principal discrete error metric is root-mean-square error (RMSE), not the continuous L2 norm:

$$\mathrm{RMSE} = \mathrm{sqrt}[(1/M)\,\Sigma(i=1,\ldots,M)\,|f(x_i)-f_h(x_i)|^2].$$

For nonsmooth tests, a post-hoc regular-region maximum error is also reported:

$$E\infty,\mathrm{reg}(\delta) = \max\{|f(x_i)-f_h(x_i)| : \mathrm{dist}(x_i,S) \geq \delta\}.$$

The known singularity set S is solely utilized for evaluation purposes, not for the adaptive construction. The omitted neighborhoods are used to calculate the max local RMS. Step test normalized overshoot and 10-90% transition width are presented. The mathematical width of the transition for the described discontinuous reconstruction is zero. Any nonzero grid crossing width is a diagnostic-resolution artifact and is hence not represented as a physical transition layer.

4. Numerical Results

4.1. Coefficient Decay and Localization

The global coefficient plots in Figure 2 show the expected hierarchy with the analytic function decaying fastest and the cusp, algebraic, jump, and mixed functions having larger high-order coefficients. This is consistent with the idea that connects the loss of regularity with the slower decay of coefficients and localized spectral error. (Liu *et al.*, 2019; Wang, 2023; Xie *et al.*, 2026) [13, 16, 17].

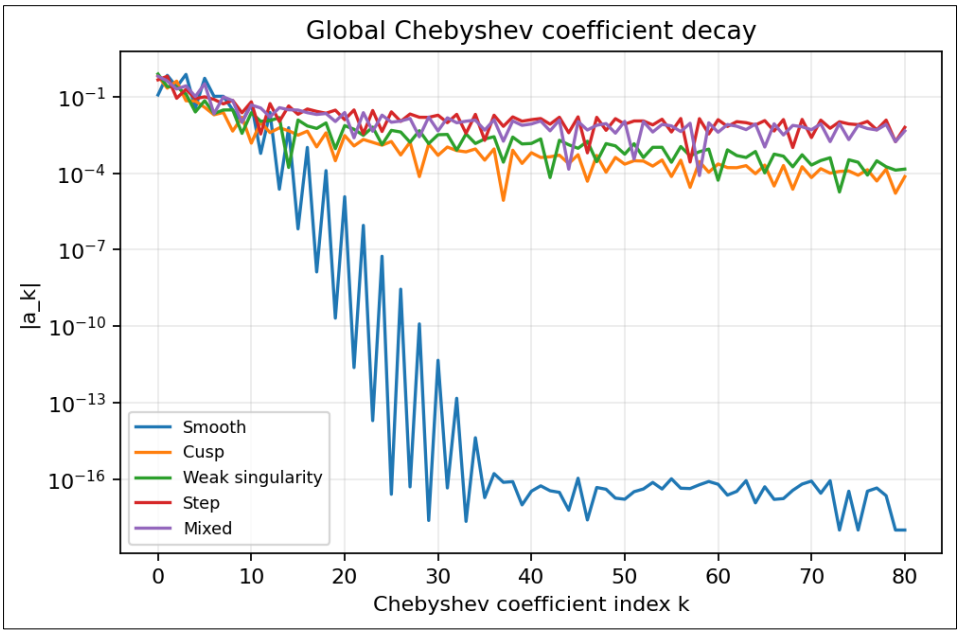


Fig 2: Global Chebyshev coefficient magnitudes for the five benchmarks.

Table 4: Localization of nonsmooth features. Jump errors are post-bracketing bisection errors.

Function	Type	True x	Reported x	|error|	Flagged width	Estimator
Cusp	cusp	0.170000	0.1679687500	2.03e-03	0.0078125	Midpoint of flagged leaf
Weak singularity	singularity	-0.330000	-0.3320312500	2.03e-03	0.0078125	Midpoint of flagged leaf
Step	jump	0.130000	0.1300000000	4.66e-12	0.0078125	Bisection after bracketing
Mixed	cusp	-0.410000	-0.4101562500	1.56e-04	0.0078125	Midpoint of flagged leaf
Mixed	jump	0.230000	0.2300000001	9.78e-11	0.0078125	Bisection after bracketing

In case dmax equals 8, the leaf, which was not resolved, has a width of 0.0078125. The leap sites are revised in a range that has been observed in the past, so the cusp estimations have the precision predicted for the leaf scale. By making this difference, the possibility of confusing the bisection tolerance with the accuracy of the first nonsmooth-feature detector is avoided. This is because it is easy to avoid the misunderstanding.

4.2. Primary Accuracy Comparison at Matched Representation Size

Three motifs emerge clearly. First, global Chebyshev is demonstrably best on the analytic benchmark, achieving machine-scale inaccuracy with just 42 coefficients; the hybrid overhead is superfluous there. Second, for the nonsmooth benchmarks, subdivision alone is not enough. Compared with the adaptive Chebyshev-only control,

switching to PCHIP decreases RMSE from 1.42×10^{-6} to 9.90×10^{-7} for the cusp and from 8.16×10^{-5} to 5.30×10^{-5} for the square-root singularity. Third, the mixed benchmark shows a substantially bigger gap: RMSE decreases from 5.24×10-3 for adaptive Chebyshev to 1.41×10-5 for the hybrid technique, while the regular-region maximum error is still 8.44×10-11 .

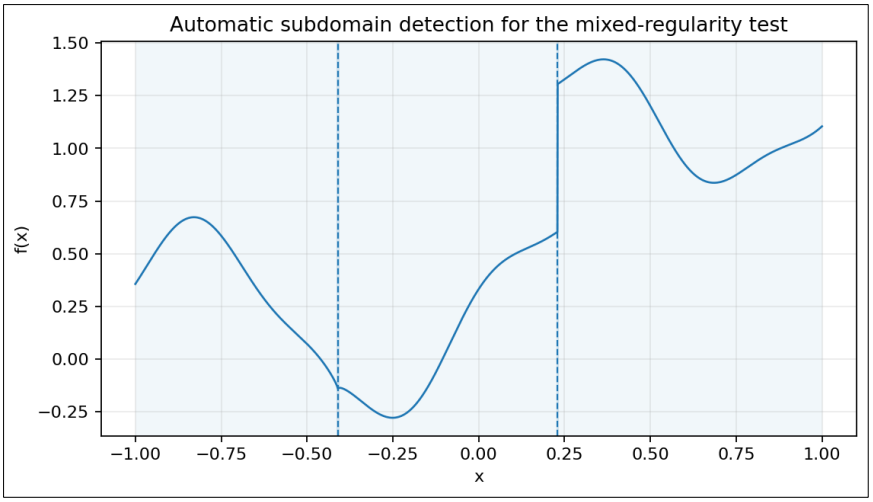


Fig 3: Automatically detected irregular subdomains in the mixed benchmark.

Table 5: Main accuracy comparison at matched stored representation size.

Function	Method	RMSE	E∞,reg	Max local RMS
Smooth	Proposed Hybrid	3.832e-12	6.860e-12	
Smooth	Adaptive Chebyshev	3.832e-12	6.860e-12	
Smooth	Global Chebyshev	4.660e-16	1.610e-15	
Smooth	Global PCHIP	1.975e-03	1.051e-02	
Smooth	Cubic Spline	3.211e-05	2.529e-04	
Cusp	Proposed Hybrid	9.900e-07	3.331e-16	7.001e-06
Cusp	Adaptive Chebyshev	1.423e-06	3.331e-16	1.006e-05
Cusp	Global Chebyshev	3.557e-04	1.551e-03	2.030e-03
Cusp	Global PCHIP	2.024e-04	2.220e-16	1.431e-03
Cusp	Cubic Spline	1.355e-04	2.562e-04	9.551e-04
Weak singularity	Proposed Hybrid	5.298e-05	1.469e-12	3.746e-04
Weak singularity	Adaptive Chebyshev	8.161e-05	1.469e-12	5.770e-04
Weak singularity	Global Chebyshev	2.228e-03	5.706e-03	1.521e-02
Weak singularity	Global PCHIP	1.965e-03	2.369e-04	1.389e-02
Weak singularity	Cubic Spline	1.660e-03	2.391e-03	1.172e-02
Step	Proposed Hybrid	1.526e-06	0.000e+00	1.079e-05
Step	Adaptive Chebyshev	7.914e-03	0.000e+00	5.596e-02
Step	Global Chebyshev	3.476e-02	1.232e-01	2.318e-01
Step	Global PCHIP	4.309e-02	0.000e+00	3.047e-01
Step	Cubic Spline	4.233e-02	2.889e-02	2.991e-01
Mixed	Proposed Hybrid	1.411e-05	8.438e-11	9.976e-05
Mixed	Adaptive Chebyshev	5.242e-03	8.438e-11	3.706e-02
Mixed	Global Chebyshev	2.282e-02	5.360e-02	1.575e-01
Mixed	Global PCHIP	2.126e-02	1.097e-04	1.503e-01
Mixed	Cubic Spline	2.089e-02	5.128e-03	1.477e-01

4.3. Physical-Space Behavior Near the Mixed Singularities

The global Chebyshev spreads the oscillatory error over the nonsmooth features. The global PCHIP avoids the global polynomial ringing but loses the high-order accuracy in the smooth oscillatory areas. The adaptive Chebyshev control localizes the tough area but still utilizes a terminal polynomial in the region. The hybrid technique, however, limits PCHIP just to the two terminal irregular leaves, and preserves Chebyshev elsewhere.

4.4. Step Benchmark: Overshoot and Edge Representation

The global Chebyshev and the terminal adaptive Chebyshev polynomial overshoot the unit step by about 14%. The cubic spline overshoots by 10.78 percent. Global PCHIP is non-oscillatory, but it substitutes the discontinuity with a finite transition layer. The suggested jump-aware design is similarly nonoscillatory, however, unlike global PCHIP, it allows a discontinuous split, therefore its mathematical 10-90% transition width is zero.

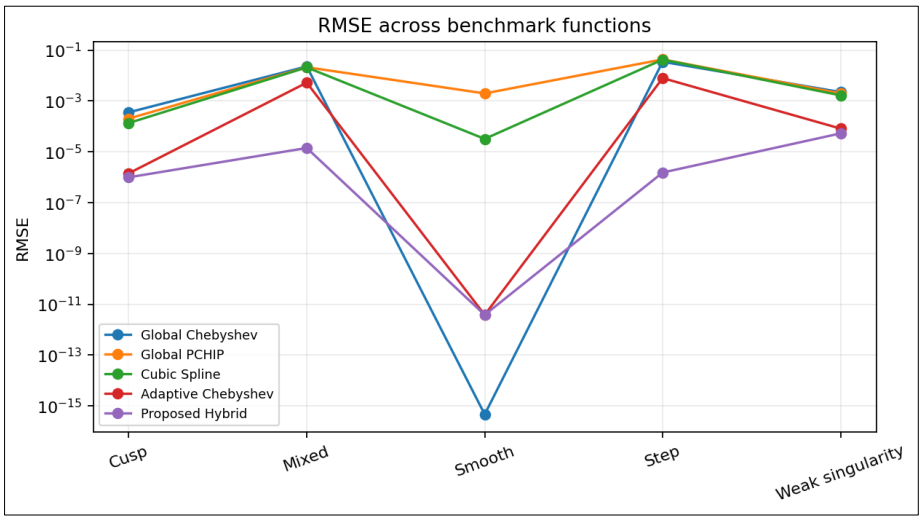


Fig 4: RMSE across the five benchmark functions.

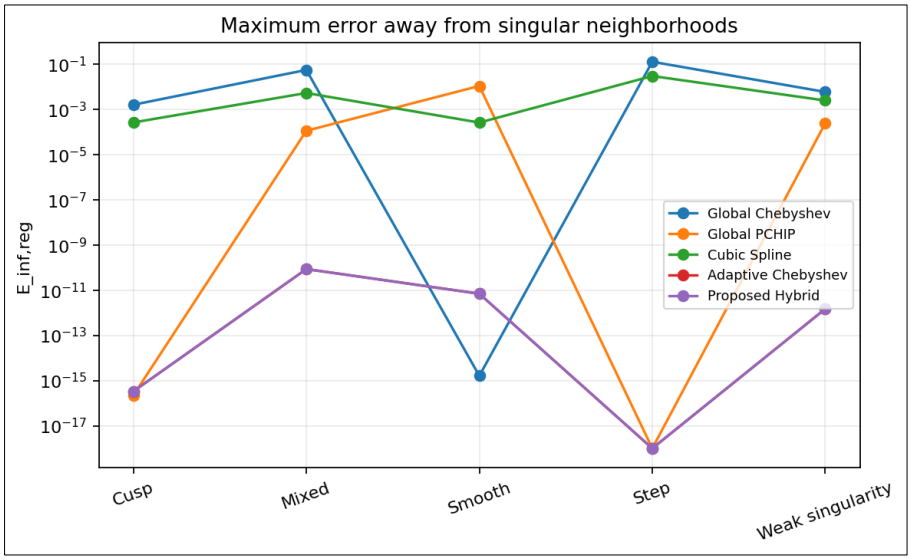


Fig 5: Maximum error outside the fixed singular neighborhoods.

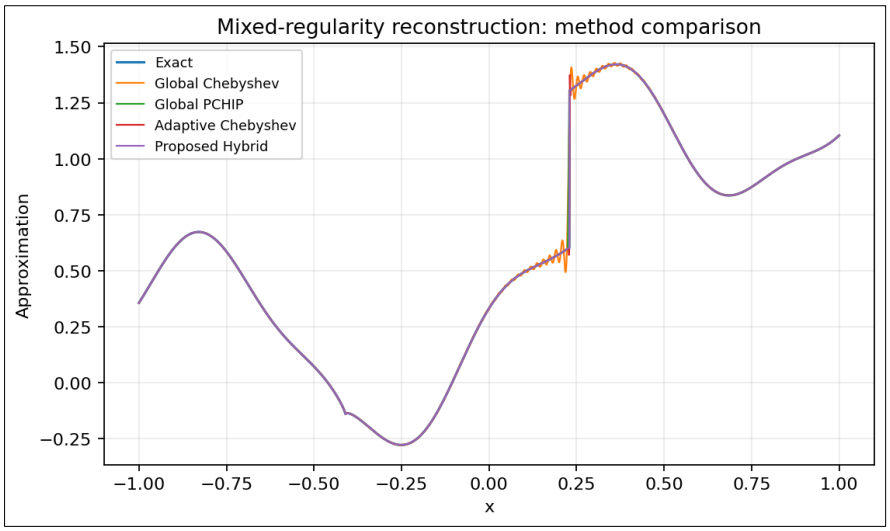


Fig 6: Full mixed-function reconstruction by the comparison methods.

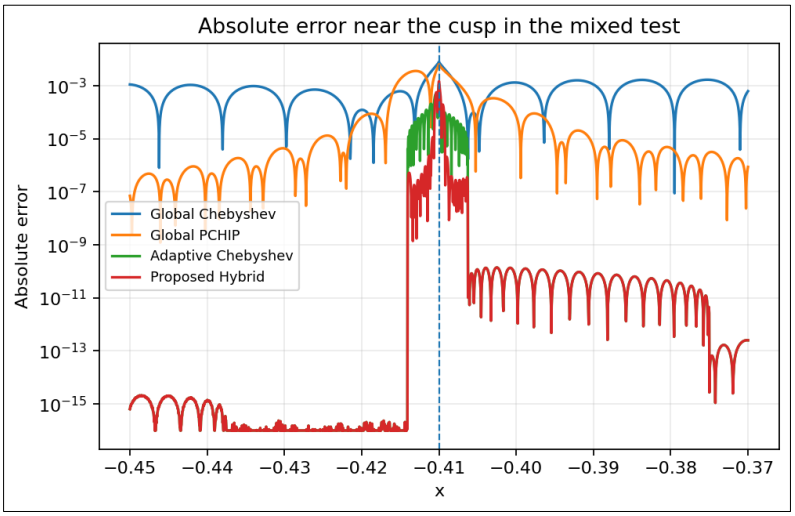


Fig 7: Absolute error near the cusp x=-0.41.

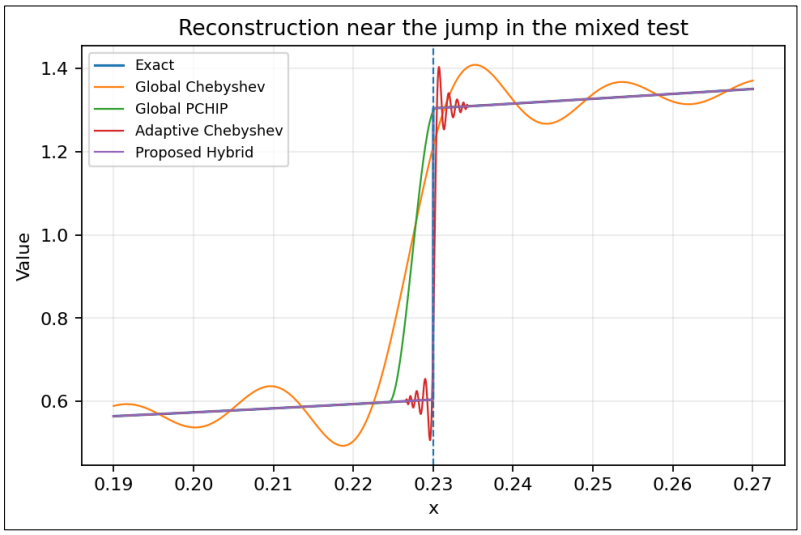


Fig 8: Reconstruction near the mixed-function jump x=0.23.

Table 6: Step-function edge metrics. The hybrid reconstruction is explicitly discontinuous at the detected split.

Method	Overshoot (%)	10-90% transition width
Proposed Hybrid	0.000	0 (discontinuous)
Adaptive Chebyshev	14.284	4.455343e-04
Global Chebyshev	14.129	1.163840e-02
Global PCHIP	0.000	6.083999e-03
Cubic Spline	10.781	7.385636e-03

4.5. Construction Cost and Equal-Evaluation-Budget Comparison

The adaptive construction is more costly than a global interpolant of the same stored size, as it uses evaluations for local coefficient testing and off-grid validation. In the mixed benchmark the hybrid representation stores 344 degrees of freedom but needs 1,317 unique function evaluations for building. This overhead is not concealed.

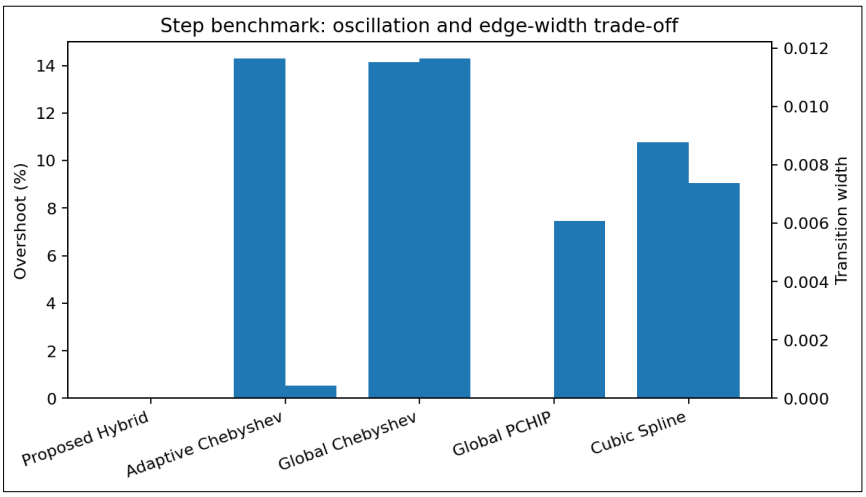


Fig 9: Step benchmark: overshoot and transition-width trade-off.

Table 7: Representation size and unique function evaluations used during construction.

Function	Method	Stored DOF	Build evaluations
Smooth	Proposed Hybrid	42	143
Smooth	Adaptive Chebyshev	42	143
Smooth	Global Chebyshev	42	42
Smooth	Global PCHIP	42	42
Smooth	Cubic Spline	42	42
Cusp	Proposed Hybrid	185	720
Cusp	Adaptive Chebyshev	189	690
Cusp	Global Chebyshev	185	185
Cusp	Global PCHIP	185	185
Cusp	Cubic Spline	185	185
Weak singularity	Proposed Hybrid	185	720
Weak singularity	Adaptive Chebyshev	189	690
Weak singularity	Global Chebyshev	185	185
Weak singularity	Global PCHIP	185	185
Weak singularity	Cubic Spline	185	185
Step	Proposed Hybrid	201	740
Step	Adaptive Chebyshev	189	690
Step	Global Chebyshev	201	201
Step	Global PCHIP	201	201
Step	Cubic Spline	201	201
Mixed	Proposed Hybrid	344	1317
Mixed	Adaptive Chebyshev	336	1237
Mixed	Global Chebyshev	344	344
Mixed	Global PCHIP	344	344
Mixed	Cubic Spline	344	344

Table 8: Mixed benchmark at the same construction budget of 1,317 function evaluations.

Method	Stored DOF	Build evals	RMSE	E∞,reg	Local RMS
Global Chebyshev	1317	1317	1.070e-02	1.237e-02	7.513e-02
Global PCHIP	1317	1317	6.000e-03	5.601e-06	4.243e-02
Cubic Spline	1317	1317	6.558e-03	9.637e-09	4.637e-02
Proposed Hybrid	344	1317	1.411e-05	8.438e-11	9.976e-05

The leveling of building budgets doesn't negate the benefit of localization. For 1,317 samples global Chebyshev has RMSE $1.07\text{x}10^{-2}$, global PCHIP $6.00\text{x}10^{-3}$ and cubic splines $6.56\text{x}10^{-3}$. The hybrid technique is at $1.41\text{x}10^{-5}$ storing just 344 degrees of freedom. This means that the mixed-function outcome is not readily explained by giving the adaptive algorithm extra black-box evaluations.

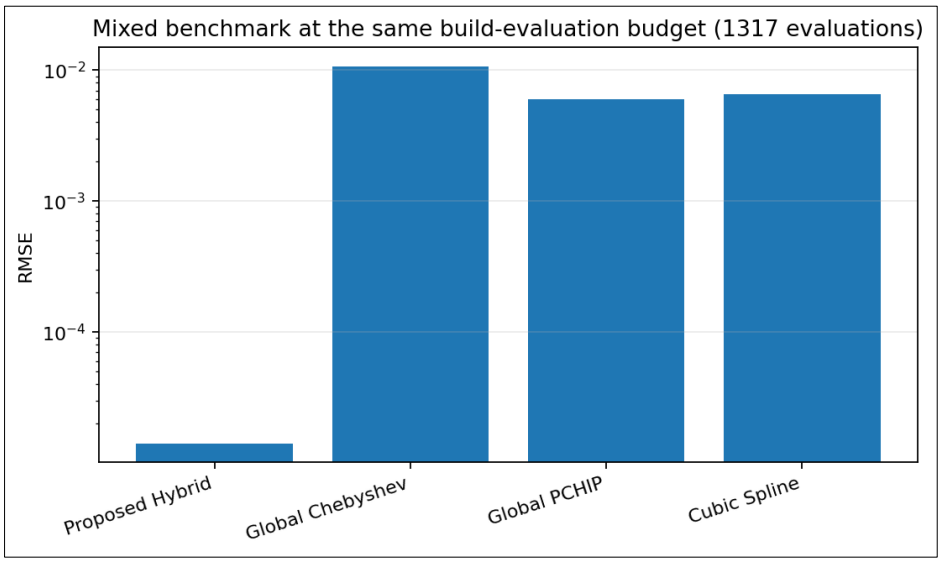


Fig 10: RMSE on the mixed benchmark at the same build-evaluation budget.

4.6. Degree, PCHIP-resolution, and Depth Sensitivity

Increasing m from 8 to 28 reduces the regular-region maximum error from 5.87×10^{-8} to 2.15×10^{-13}, while RMSE remains approximately 1.41×10^{-5}. The remaining global error is therefore controlled by the localized irregular neighborhoods, not by the smooth Chebyshev regions.

Table 9: Sensitivity to local Chebyshev degree on the mixed benchmark.

m	Leaves	DOF	Build evals	RMSE	E∞,reg
8	26	266	857	1.411e-05	5.867e-08
12	18	258	863	1.411e-05	4.297e-08
16	16	288	1060	1.411e-05	1.816e-09
20	16	344	1317	1.411e-05	8.438e-11
24	16	400	1529	1.411e-05	4.168e-12
28	16	456	1816	1.411e-05	2.149e-13

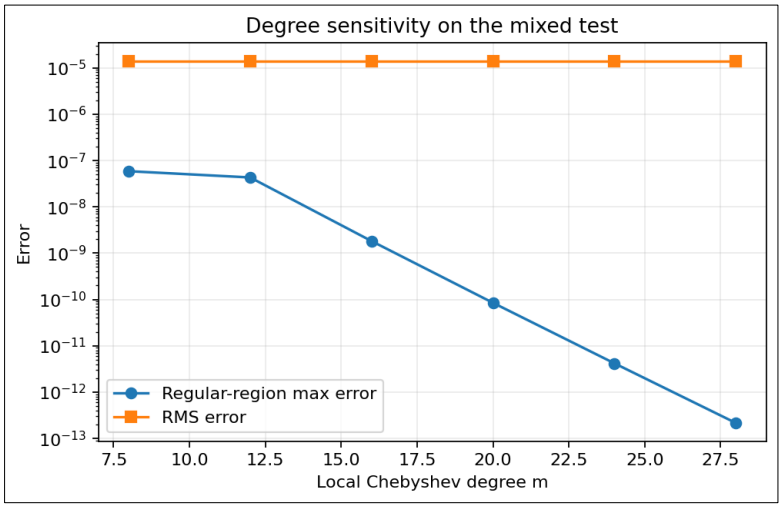


Fig 11: Local Chebyshev degree mainly controls smooth-region accuracy.

Table 10: Sensitivity to local PCHIP resolution.

PCHIP nodes	DOF	Build evals	RMSE	Max local RMS
5	332	1317	4.506e-05	3.187e-04
9	336	1317	2.156e-05	1.524e-04
17	344	1317	1.411e-05	9.976e-05
33	360	1317	5.239e-06	3.705e-05
65	424	1381	2.423e-06	1.714e-05

Increasing the PCHIP nodes from 5 to 65 lowers mixed-function RMSE from 4.51×10^{-5} to 2.42×10^{-6} and local RMS from 3.19×10^{-4} to 1.71×10^{-5}. This confirms that the dominant residual error belongs to the terminal irregular neighborhoods.

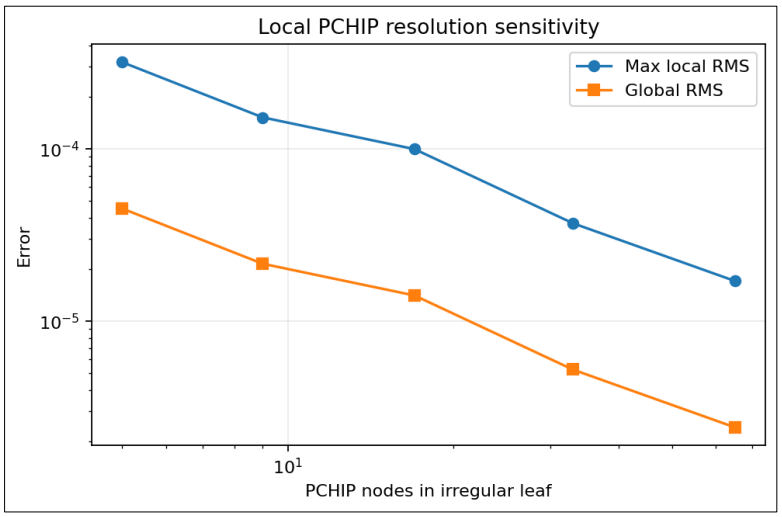


Fig 12: Sensitivity to local PCHIP resolution.

Table 11: Recursive-depth sensitivity.

dmax	Leaves	DOF	Build evals	RMSE	E∞,reg	Local RMS
5	10	218	849	1.134e-04	3.566e-06	8.018e-04
6	12	260	1005	4.495e-05	3.121e-07	3.179e-04
7	14	302	1161	2.156e-05	8.438e-11	1.524e-04
8	16	344	1317	1.411e-05	8.438e-11	9.976e-05
9	18	386	1473	4.666e-06	8.438e-11	3.299e-05

Depth is the most visible accuracy-cost trade-off knob. Increasing dmax from 5 to 9 resulted in the number of construction evaluations increasing from 849 to 1,473, while at the same time the root mean square error (RMSE) decreasing from 1.13×10^{-4} to 4.67×10^{-4}. The deeper the refinement, the more the problematic areas are narrowed and therefore the prevailing nonsmooth error is minimized compared to the degree of the local polynomial.

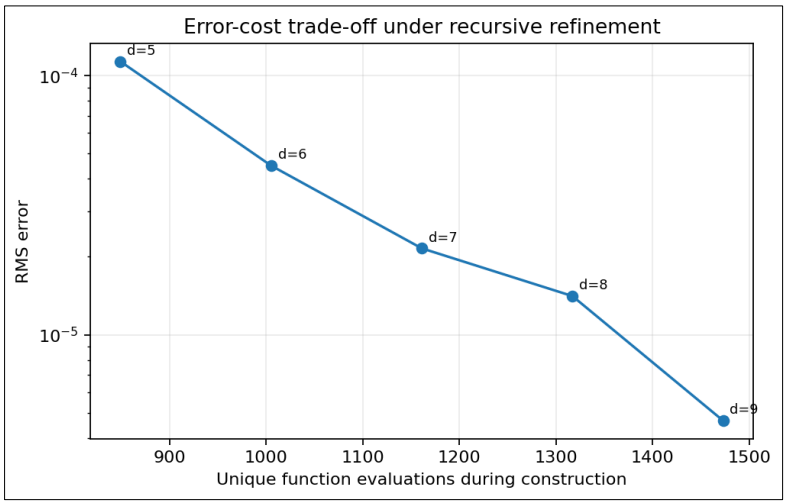


Fig 13: RMSE versus construction cost under increasing recursive depth.

4.7. Detector-Parameter and Jump-Classifier Robustness

The mixed benchmark is insensitive to tau for more than two orders of magnitude and to q from 3 to 8. This is not intended to imply that the parameters are always insensitive. Here the terminal judgments are dominated by the off-grid validation residual and the recursive depth, so the tail threshold is not the active restriction across the range examined. However, the finding is helpful, in that it indicates that the baseline results are not the artifact of a carefully calibrated tau or q.

Table 12: Robustness of the mixed benchmark to coefficient-tail settings.

Parameter	Tested range	Leaves	DOF	RMSE	Observed effect
Tail threshold tau	3e-5 to 1e-2	16	344	1.411e-5	Partition and errors unchanged
Tail terms q	3 to 8	16	344	1.411e-5	Partition and errors unchanged

Table 13: Selected jump-threshold robustness tests. "Yes" means at least one terminal leaf was classified as a jump.

Test	J*=4	J*=8	J*=16	J*=24
Step	Yes	Yes	Yes	Yes
Cusp	No	No	No	No
Weak singularity	No	No	No	No
Steep tanh	No	No	No	No
High-frequency sine	No	No	No	No
Narrow Gaussian	No	No	No	No

Deterministic tests never identify the cusp, square-root singularity, steep tanh layer, high-frequency sine, or narrow Gaussian as a jump, but always identify the unit step as a jump for J*=4 to 24. This is a negative control test, not a demonstration that the classifier is reliable on random data or noise.

Table 14: Jump-location and amplitude robustness for 20 piecewise-constant tests.

True jump x	Amplitude range	Detected	Max post-bracketing |error|
-0.61	0.25-2.00	4/4	1.40e-11
-0.23	0.25-2.00	4/4	9.78e-11
0.13	0.25-2.00	4/4	4.66e-12
0.37	0.25-2.00	4/4	4.66e-12
0.71	0.25-2.00	4/4	7.92e-11

The jumps were refined after automated bracketing and polishing of all twenty piecewise constant leaps. The biggest error in the post-bracketing position was seen to be 9.78×10^{-11}. The same bracketing behavior is obtained for all four different amplitudes examined in these noiseless step tests. This is because the leap score is standardized on a median first-difference scale.

4.8. Sensitivity to the Post-Hoc Exclusion Radius

The exclusion radius is used just to provide an overview of inaccuracy away from previously known singularities once the approximation has been established. The baseline option delta=0.02 does not provide the principal ranking since the proposed method has the shortest regular-region maximum error among the global comparison strategies spanning delta=0.01, 0.02, and 0.04.

Table 15: Mixed-benchmark regular-region maximum error under three exclusion radii.

delta	Proposed Hybrid	Global Chebyshev	Global PCHIP	Cubic Spline
0.01	1.277e-10	9.892e-02	2.433e-04	3.415e-02
0.02	8.438e-11	5.360e-02	1.097e-04	5.128e-03
0.04	4.316e-11	2.455e-02	1.097e-04	2.792e-05

5. Discussion

The results favor a conditional, regularity-aware account rather than a universal ranking. As predicted by classical spectral theory, global Chebyshev interpolation performs better when the whole function is analytic. If the function has smooth and nonsmooth segments, the hybrid approach prevents a local fault from dominating the approximation family throughout the interval. Theoretical studies showing slower decay of Chebyshev coefficients and localization of errors near singularities support this perspective (Liu *et al*., 2019; Wang, 2023; Xie, 2026) [13, 16, 17].

The evidence is focused on adaptive Chebyshev-only control. The same recursive division approach is employed, thus the gains are not only from identifying the challenging region. The last distinction is the family of local representations. For cusps and algebraic singularities, PCHIP produces somewhat but reliably reduced local and global RMS error. The global PCHIP is everyplace continuous in the domain and it smooths jumps, however it is non-oscillatory. More important than form preservation is the possibility of making a discontinuous one-sided reconstruction.

The practical argument is supported by the equal-evaluation-budget experiment. Even with all 1,317 adaptive build samples available, global techniques are orders of magnitude less accurate on the mixed benchmark. Thus, local regularity promotes representational complexity, not sample size. But the hybrid solution should not be sold as a cheap universal default. The smooth benchmark shows that direct global Chebyshev interpolation is preferable provided one knows a priori that the function is globally analytic. It takes a lot of money to build.

Jump tests show promise deterministic robustness but are limited in scope. The classifier can distinguish a classical step from many non-jump controls across a wide range of thresholds, and automatic bracketing works at five jump locations and four amplitudes. Bisection makes relatively little faults in location after good bracketing. No performance for aliased, noisy or under-sampled data. Noise is required as high-order coefficients and finite-difference medians might be distorted, resulting in spurious irregularity or jump decisions.

The study has two additional limitations. First, the validation residual is sampled on a finite off-grid set and therefore does not provide a rigorous a posteriori supremum-norm certificate. A narrow unresolved feature could, in principle, lie between validation points. Second, the algorithm is one-dimensional (Akansha, 2024a; Akansha, 2025) [1, 3].

6. Conclusions

A validation-guided Chebyshev-PCHIP approximation was tested on analytic, cusp, algebraic-singularity, jump, and mixed-regularity functions. Local Chebyshev interpolation is allowed only if coefficient decay and off-grid validation are sufficient. It iteratively narrows unresolved areas and switches terminal irregular leaves to PCHIP. A separate jump classifier allows one-sided PCHIP pieces to keep the final representation discontinuous when data suggest a real leap.

Not all numbers show that the hybrid technique is better. Analytic control should use global Chebyshev. The hybrid advantage occurs when regularity is spatially diverse. The technique achieves RMSE 1.41×10^{-5} and regular-region maximum error 8.44×10^{-11} on the mixed benchmark, whereas adaptive Chebyshev has RMSE 5.24×10^{-3} and global alternatives have around $2\text{x}10^{-2}$ at matching stored size. When global techniques get the same 1,317 construction assessments, the advantage remains.

Sensitivity experiments separate primary parameter roles. PCHIP node count regulates residual error in irregular leaves, local Chebyshev degree governs smooth-region precision, and recursive depth controls the primary accuracy-cost trade-off. The baseline mixed partition and jump classifier are stable throughout tail-threshold and tail-length ranges for the deterministic positive and negative controls.

Future work should derive a rigorous a posteriori bound using local Chebyshev tail information, validation residuals, and PCHIP interpolation error, compare the simple tail ratio directly with standard coefficient-chopping rules, introduce noise-aware thresholds, and extend the switching principle to multidimensional decompositions.

Data and Reproducibility Statement

Section 3 provides deterministic benchmark methods for all results. A type-I discrete cosine transform computes Chebyshev coefficients from Chebyshev-Lobatto points. The error metrics use 200,000 midpoint samples on [-1,1]. The number of unique black-box samples equals the building cost since abscissa caches function evaluations. Baseline: Python 3.13.5, NumPy 2.3.5, SciPy 1.17.0, pandas 2.2.3, Matplotlib 3.10.8. No external data were used.

References

1. Akansha S. Decay analysis of bivariate Chebyshev coefficients for functions with limited regularity. Results in Applied Mathematics. 2024;22:100449. doi:10.1016/j.rinam.2024.100449
2. Akansha S. Piecewise nonlinear approximation for non-smooth functions. Results in Applied Mathematics. 2024;23:100491. doi:10.1016/j.rinam.2024.100491
3. Akansha S. Padé-based nonlinear approximation of bivariate non-smooth functions. BIT Numerical Mathematics. 2025;65:17. doi:10.1007/s10543-025-01059-8
4. Akansha S, Subramaniam A. Exploring Chebyshev polynomial approximations: Error estimates for functions of bounded variation. AIMS Mathematics. 2025;10(4):8688-8706. doi:10.3934/math.2025398
5. Aurentz JL, Trefethen LN. Chopping a Chebyshev series. ACM Transactions on Mathematical Software. 2017;43(4):33. doi:10.1145/2998442
6. Baeza A, Donat R, Martínez-Gavara A. On the use of monotonicity-preserving interpolatory techniques in multilevel schemes for balance laws. Communications on Applied Mathematics and Computation. 2024;6:1319-1341. doi:10.1007/s42967-023-00332-3
7. Berrut JP, Trefethen LN. Barycentric Lagrange interpolation. SIAM Review. 2004;46(3):501-517. doi:10.1137/S0036144502417715
8. Driscoll TA, Weideman JAC. Optimal domain splitting for interpolation by Chebyshev polynomials. SIAM Journal on Numerical Analysis. 2014;52(4):1913-1927. doi:10.1137/130919428
9. Drozd K, Furfaro R, D'Ambrosio A. A Theory of Functional Connections-based hp-adaptive mesh refinement algorithm for solving hypersensitive two-point boundary-value problems. Mathematics. 2024;12(9):1360. doi:10.3390/math12091360
10. Fritsch FN, Butland J. A method for constructing local monotone piecewise cubic interpolants. SIAM Journal on Scientific and Statistical Computing. 1984;5(2):300-304. doi:10.1137/0905021
11. Fritsch FN, Carlson RE. Monotone piecewise cubic interpolation. SIAM Journal on Numerical Analysis. 1980;17(2):238-246. doi:10.1137/0717021
12. Huynh HT. Accurate monotone cubic interpolation. SIAM Journal on Numerical Analysis. 1993;30(1):57-100. doi:10.1137/0730004
13. Liu W, Wang LL, Li H. Optimal error estimates for Chebyshev approximations of functions with limited regularity in fractional Sobolev-type spaces. Mathematics of Computation. 2019;88(320):2857-2895. doi:10.1090/mcom/3456
14. Pachón R, Platte RB, Trefethen LN. Piecewise-smooth chebfuns. IMA Journal of Numerical Analysis. 2010;30(4):898-916. doi:10.1093/imanum/drp008
15. Trefethen LN. Approximation Theory and Approximation Practice (Extended ed.). SIAM; 2019. doi:10.1137/1.9781611975949
16. Wang H. Analysis of error localization of Chebyshev spectral approximations. SIAM Journal on Numerical Analysis. 2023;61(2):952-972. doi:10.1137/22M1481452
17. Xie R, Liu W, Wu B. Sharp pointwise error estimates for Chebyshev approximations of functions with singularities in fractional spaces. Journal of Approximation Theory. 2026;318:106307. doi:10.1016/j.jat.2026.106307
18. Zhang X, Boyd JP. Asymptotic coefficients and errors for Chebyshev polynomial approximations with weak endpoint singularities: Effects of different bases. Science China Mathematics. 2023;66(1):191-220. doi:10.1007/s11425-021-1974-x

Appendix A. Implementation Details

For each candidate interval, Chebyshev-Lobatto samples are evaluated through a cache so shared endpoints are not counted twice. The type-I DCT is normalized to return coefficients in the standard first-kind Chebyshev basis. The validation set contains 2m+1 interior equally spaced points. At a terminal irregular leaf, the jump classifier uses 33 equally spaced local samples. If the jump score exceeds J*,

the largest first difference supplies a bracket and 20 bisection steps refine the split using the midpoint of the two bracketing levels as the decision level. A non-jump irregular leaf uses 17 equally spaced PCHIP nodes in the baseline run.

An adaptive constructor is never given known singularity locations. The E$^\infty$,reg and local RMS readings are computed only after construction. The continuous L2 measure is not affected by a discontinuous benchmark at the single jump point, but a discrete grid might be affected if sampled exactly. Midpoint grids help you avoid this. The proposed step reconstruction has a zero error grid. This is because the projected split differs from the actual leap by less than one grid spacing. The study provides the continuous mismatch estimate $\sqrt{|{\Delta}x|/2}$ for the unit step when a nonzero scalar RMSE is required

How to Cite This Article

Yasari HHO. Coefficient-Guided Chebyshev–PCHIP approximation for Mixed-Regularity functions. Int J Eng Comput Appl. 2025;1(6):70-82.
doi:10.54660/.IJECA.2025.1.6.70-82.

Creative Commons (CC) License

This is an open access journal, and articles are distributed under the terms of the Creative Commons Attribution-NonCommercial-ShareAlike 4.0 International (CC BY-NC-SA 4.0) License, which allows others to remix, tweak, and build upon the work non-commercially, as long as appropriate credit is given and the new creations are licensed under the identical terms.